Summary of Machine Design and Current Regulation for the Parallel DPNV Bearingless Motor Winding

Nathan Petersen, Anvar Khamitov, Timothy Slininger, and Eric L. Severson

Department of Electrical and Computer Engineering, University of Wisconsin-Madison, WI, USA
eric.severson@wisc.edu

Abstract

This paper provides a summary of investigations into the design of combined windings and precision current regulation techniques for bearingless motors. The parallel dual-purpose, no-voltage (DPNV) winding topology is used to realize both torque and force creation. For significant power applications, it is often advantageous to implement suspension operation independent of the main motor drive. This paper shows that reasonable decoupled operation (force and torque) of combined windings using independent drives is possible through two means: 1) careful design of winding parameters such as number of slots, poles, winding factors, and geometric parameters, 2) careful current regulator design to reject disturbance voltages between the suspension and torque systems. For drives that are not independent (i.e., can transmit data between suspension and torque controllers in real-time), this paper shows that a controls-based direct voltage decoupling approach can be used to ideally decouple force and torque creation. To achieve the highest power density of the bearingless motor, the paper shows that the decoupling approach should be used. Analytical, simulation, and experimental results are presented to verify the results.

Keywords: combined winding, winding design, current regulation, bearingless motor.

This paper summarizes the key contributions from [1].

1 Introduction

Bearingless (self-bearing) motors are machines with the ability to generate both forces and torque. In this paper, radial force bearingless motors are considered for the application of levitating the rotor. Historically, these machines used two separate windings: a "torque" winding and a "suspension" winding. More recently, clever machine designers make use of combined windings where one winding creates both torque and force. The combined winding allows the drive to dynamically allocate slot current to either force or torque, depending on the system needs. This improves slot space utilization, leading to more power dense bearingless motors.

This paper studies the parallel dual-purpose no-voltage (DPNV) bearingless motor winding, depicted in Figure 1a. There are two terminal sets: three-phase torque terminals and three-phase suspension terminals. Reference [1] derives the electrical model of the parallel DPNV winding; the result is depicted in Figure 1b. In the circuit, the torque inverter $\vec{v}_t$ creates torque currents $\vec{i}_t$ which are responsible for standard motoring operation. The suspension inverter $\vec{v}_s$ injects currents into the "negative" side of coil group a which act to create forces for levitation.

Unfortunately, due to the winding topology, there is inherent cross-coupling between force and torque generation – by flowing currents which create force, inadvertently, torque will be created. Reference [1] derives this in detail from an electrical prospective. Intuitively, this can be observed by noticing that half of the suspension voltage $\vec{v}_s$ appears in the torque system circuit. The suspension operation directly creates a voltage disturbance in the torque system which, if not fully rejected, will create extraneous torque currents which can cause torque ripple.

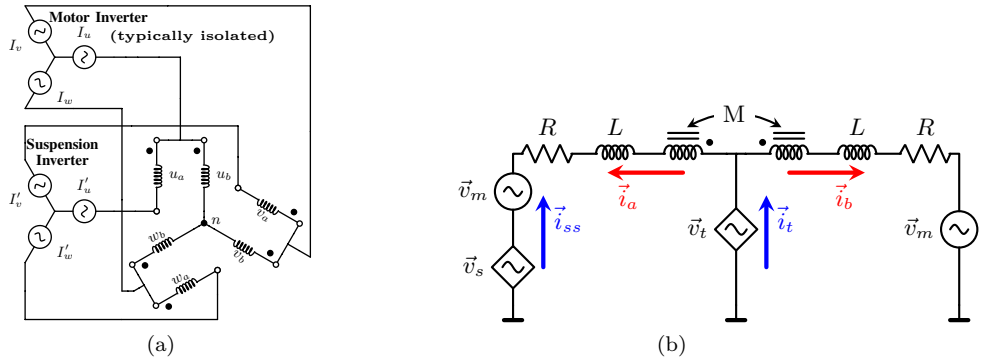

Figure 1: Parallel DPNV winding (a) drive connections (b) space vector equivalent circuit.

The amount of voltage disturbance acting from the suspension to torque system is defined as $\vec{v}_{cs}$. The $\vec{i}_t$ current regulator must reject the disturbance voltage $\vec{v}_{cs}$ in order to eliminate electrical cross-coupling. Reference [1] first derives analytical expressions for $\vec{v}_{cs}$ in terms of the machine design parameters. It is shown that, indeed, all designs which can create force inherently also create $\vec{v}_{cs}$. However, some designs are preferable due to lower cross-coupling. Overall, the magnitude of $\vec{v}_{cs}$ is entirely determined by the machine design. By carefully designing the machine, $\vec{v}_{cs}$ can be minimized.

While all machine designs will exhibit some electrical cross-coupling $\vec{v}_{cs}$ due to force generation, the overall impact of the cross-coupling is determined by the controls implementation. If no real-time communication between the the suspension and torque current regulators is possible, the overall response of the $\vec{v}_{cs}$ cross-coupling is determined by the torque current regulator's disturbance rejection capabilities. However, when real-time communication is possible (e.g., both current regulators are implemented in the same processor), direct electrical decoupling is possible to entirely eliminate the $\vec{v}_{cs}$ effects.

2 Machine Design

The voltage cross-coupling term $\vec{v}_{cs}$ is proportional to the product of the suspension currents $\vec{i}_s$ and the winding impedance $\bar{z}_s$. The required suspension current $\vec{i}_s$ is determined by the force requirement through the force proportionality constant $\bar{k}_i$ since $\vec{F} = \bar{k}_i \vec{i}_s$. Therefore, by understanding how the machine design impacts both $\bar{z}_s$ and $\bar{k}_i$, insight can be given towards minimizing $\vec{v}_{cs}$. Reference [1] provides a detailed derivation of normalized versions of both the winding impedance z_{sn} and force constant k_{in}. Normalization allows two candidate machine designs to be compared directly in terms of suspension/torque pole-pairs and winding factors. To minimize the voltage cross-coupling $\vec{v}_{cs}$, the winding impedance z_{sn} should be minimized while the force constant k_{sn} should be maximized. Unfortunately, it is shown that the two performance metrics are in conflict: $z_{sn} \propto k_{in}^2$.

To further study the performance metrics z_{sn} and k_{in}, 17 unique bearingless motors are designed and analyzed. Each machine is designed with a different number of slots, number of slots/pole/phase, and coil span. The rated specification for all machines is: 50 kW power, 30 kRPM speed, 480 Vrms line-to-line back-EMF, 0.7 T magnetic loading, and 75 kArms/m electric loading. Figure 2a shows the performance metrics of the designs, relative to Design 1. Notice that the magnitude of the voltage cross-coupling $|\vec{v}_{cs}|_n$ varies widely between designs. For details about each design variant, refer to [1].

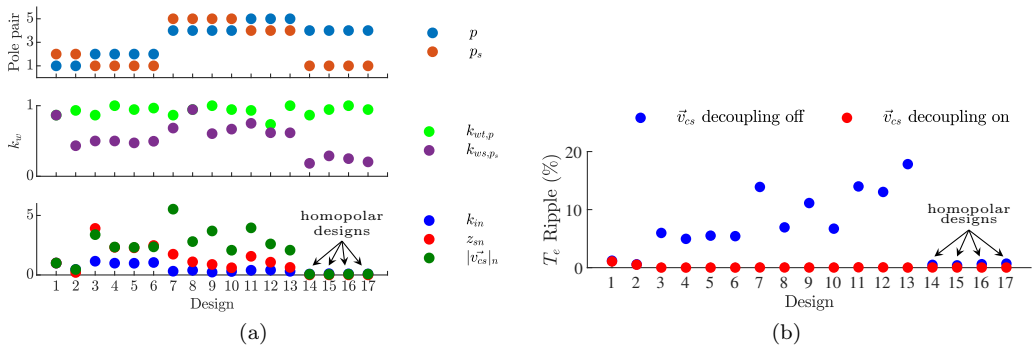

Figure 2: Various bearingless motor design performance metrics: (a) metrics based on machine design (b) resulting torque ripple due to current regulation capabilities.

3 Current Regulation

The machine design directly determines the voltage cross-coupling between the force and torque systems via $\vec{v}_{cs}$. However, the true impact of $\vec{v}_{cs}$ is entirely determined by the controls implementation. Precision current regulation is required to achieve ideal decoupling between force and torque creation. Even if real-time decoupling is not possible due to independence between motoring and suspension operation, the force-induced torque ripple can still be minimized by improving the disturbance rejection capabilities of the torque current regulator.

Figure 2b shows the simulated torque ripple of the 17 designs from Figure 2a when operating at rated speed, rated torque, and supporting the rotor weight. Standard synchronous frame PI current regulation is implemented in the discrete-time controller (referred to as SFPI). When direct electrical decoupling is used, the force-induced torque ripple vanishes. However, without decoupling, the torque ripple rises to nearly 20% for some designs.

Bearingless motors have the greatest advantage over conventional motors when operating at ultra high speeds. For precise actuation of both force and torque at these high speeds, direct digital current regulation must be deployed. Reference [1] derives the direct digital complex vector current regulator (referred to as CVCR). Theoretically, the CVCR completely decouples the rotational speed from the current regulation capability, thus enabling ultra high speeds. Figure 3 shows simulation results which compares SFPI vs. CVCR for high speed operation. Notice the deviations in the suspension currents $i_{\mathrm{s,xy}}$ at increasing speeds.

4 Experimental Results

The proposed precision current regulation techniques are implemented on an experimental bench for validation. Two prototype machines are used: 1) RL load configured as a parallel DPNV winding, 2) bearingless ac homopolar motor. First, the RL load is used. Figure 4 shows experimental results of the CVCR controlling currents at 1 kHz fundamental frequency with 1 kHz bandwidth and the controller digital sample rate of 10 kHz. With $\vec{v}_{cs}$ decoupling, the torque currents $i_{\mathrm{t,dq}}$ are not affected by the step changes in the suspension currents $i_{\mathrm{s,xy}}$. However, without $\vec{v}_{cs}$ decoupling, excessive torque current ripple occurs.

Finally, the proposed current regulation techniques are implemented to levitate and rotate the ac homopolar bearingless motor. Figure 5 shows the torque and suspension currents in their respective synchronous reference frame. Notice that, with no $\vec{v}_{cs}$ decoupling, the torque currents $i_{\mathrm{t,dq}}$ show noticeable ripple which vanishes when decoupling is enabled.

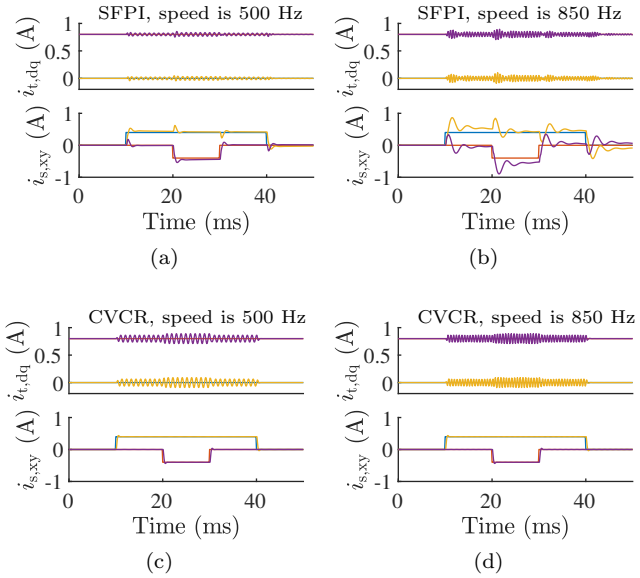

Figure 3: Simulated current regulation (torque $i_{\mathrm{t,dq}}$ and suspension $i_{\mathrm{s,xy}}$) comparing the Synchronous Frame PI (SFPI) controller with the Complex Vector Current Regulator (CVCR).

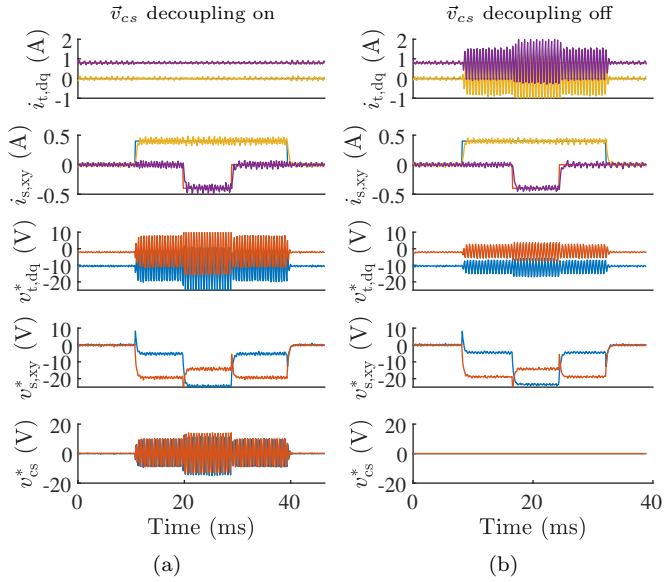

Figure 4: Experimental results of current regulation on the RL load using the proposed CVCR.

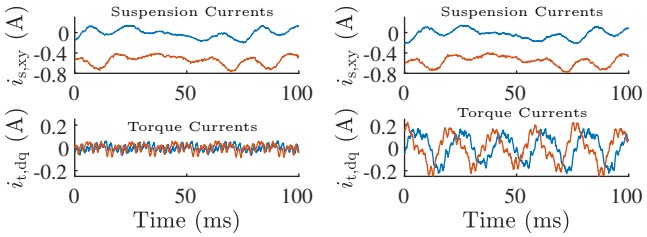

Figure 5: AC homopolar motor operating with CVCR and $\vec{v}_{cs}$ decoupling: (a) on (b) off.

5 Conclusion

This paper summarizes the contributions of Reference [1]. The parallel dual-purpose no-voltage (DPNV) combined winding bearing motor topology is investigated in detail. The electrical cross-coupling between the force and torque systems is the key topic; the paper proposes solutions to reduce or eliminate the cross-coupling. It is shown that careful machine design can result in reduced cross-coupling, however, the controls implementation ultimately determines the overall impact of the force-induced cross-coupling. The motoring current regulator's disturbance rejection properties are directly responsible for reducing the force-induced torque ripple. If real-time communication between the suspension and torque current controllers is possible, direct electrical decoupling is possible. Overall, the paper highlights the need for codesign of both the machine and controls to achieve the best bearingless motor solution.

References

[1] Nathan Petersen, Anvar Khamitov, Timothy Slininger, and Eric Loren Severson. Machine design and precision current regulation for the parallel dpnv bearingless motor winding. *IEEE Transactions on Industry Applications*, pages 1–1, 2021.